

# Dislocation loop dynamics in freestanding smectic films: The role of the disjoining pressure and of the finite permeability of the meniscus

P. Oswald, F. Picano, and F. Caillier

*Ecole Normale Supérieure de Lyon, Laboratoire de Physique, C.N.R.S. UMR5672, 46 Allée d'Italie, 69364 Lyon Cedex 07, France*

(Received 23 June 2003; published 3 December 2003)

When a dislocation loop nucleates in a freestanding film, it collapses or grows depending on whether its radius  $r$  is smaller or larger than a critical radius  $r_c$ . In this paper, we analyze the growth dynamics of a dislocation loop in the limit of  $r \gg r_c$ . Experiments with pure octylcyanobiphenyl show that the dislocation velocity is constant in thick films (more than 100 layers) regardless of their thicknesses, and only depends on the pressure in the meniscus. At intermediate thickness (between 100 and 15 layers), the velocity is no longer constant and tends to decrease in time on account of the finite permeability of the meniscus. In very thin films (less than 15 layers), the dislocations move faster than in thick films, although their velocities continue to decrease in time. The thinner the film, the larger the global acceleration is. This effect is linked to a supplementary force acting on the dislocations caused by the attraction between the free surfaces (where the smectic order parameter is enhanced). The progressive deceleration is due to the finite permeability of the meniscus.

DOI: 10.1103/PhysRevE.68.061701

PACS number(s): 61.30.Jf

## I. INTRODUCTION

Smectic-*A* phases consist of rodlike molecules arranged in fluid layers with perpendicular orientation [1]. In freestanding films, these layers are perfectly parallel to the free surfaces [2]. When a film is stretched on a frame, a large number of circular steps nucleate, separating regions with different thicknesses [3]. The steps (which are dislocations located in the middle of the freestanding film [4]) initially form patterns very similar to two-dimensional (2D) foams [3]. More important, the film is attached to its frame via a meniscus of volume usually much larger than that of the film itself from this point of view, the meniscus acts as a reservoir of matter. Microscope observations show that the initial texture is unstable and slowly evolves towards a film of constant thickness surrounded by a meniscus of circular profile and of constant cross-sectional area [3,5,6]. In this metastable state, the film can survive for a very long time (many months in a very clean atmosphere, provided that the liquid crystal does not spread out on its frame). The final thickness of the film can vary between three and many thousands of layers depending on its stretching velocity: the larger this velocity, the thinner the film is. In addition, a film systematically tends to get thinner. Suppose a dislocation loop nucleates; if the film is thinner inside the loop than outside (pore), the latter will systematically grow provided that its initial radius is larger than a critical radius. In practice, this critical radius of nucleation is a few tens of micrometer in the range of temperature in which the bulk smectic phase exists [5,6]. This value results from the balance between the line tension of the dislocation [7] (which makes the loop collapse) and the driving force due to both the pressure drop  $\Delta P = P_{air} - P_{film}$  between the air and the interior of the film and the attraction between the two free surfaces [8–10]. It turns out that when the pore radius  $r$  is much larger than  $r_c$ , the line tension force can be neglected with respect to both the driving force and the viscous force that the line experiences when it propagates inside the film.

The goal of this paper is to analyze the loop dynamics in the regime  $r > r_c$  both theoretically and experimentally. This problem was already tackled theoretically in a recent paper [11] in the limit of thick films (for a review, see also Ref. [12]). It was shown that the meniscus does not behave as a perfect reservoir, i.e., does not impose the pressure inside the film because of its finite permeability (dissipative reservoir). In other words, a pressure difference must exist between the interior of the film and the bulk of the meniscus when there is a flow of matter between them. It was predicted that this effect should lead to a significant decrease of the growth velocity of the loop as its radius increases and approaches that of the meniscus. In the previous paper the influence of surface ordering and of the interactions between the free surfaces was neglected. It turns out that this second effect sometimes adds to that of finite meniscus permeability and makes the dynamics more complicated, especially in very thin films (less than ten layers, typically) [10].

In this paper, we analyze theoretically in Sec. II the influence of these two effects when they act together and we predict the time evolution of a dislocation loop as a function of film thickness. In Sec. III, we report our experimental results obtained with 4-*n*-octyl-cyanobiphenyl (8CB) films. In Sec. IV, we fit our experimental findings to the theoretical predictions and determine the permeability constant of the meniscus. We then compare in Sec. V smectic films with soap films obtained from concentrated micellar solutions, in which similar phenomena occur. In particular, we stress the similarities and differences of the dynamical behaviors of these two kinds of films. We conclude in Sec. VI.

## II. DISLOCATION LOOP DYNAMICS: THEORY

The geometry of the experiment is shown in Fig. 1. As explained in Ref. [11], there are two equivalent ways to treat the problem of loop dynamics. The first one is to use a local approach that considers the forces affecting the line. The second approach, which we will use for convenience in the following, is global and is based on the dissipation theorem

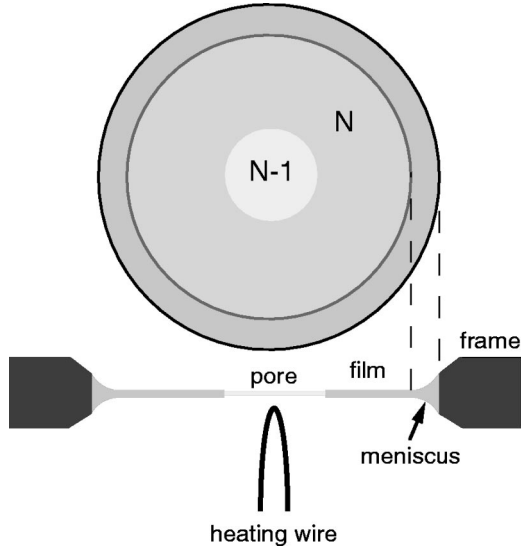


FIG. 1. Geometry of the experiment. A dislocation loop is nucleated with the help of a small heating wire in a circular freestanding film surrounded by a meniscus.

which we apply to the whole system—the film and meniscus. It consists of balancing the free energy gained by the system to the energy dissipated during loop growth:

$$\frac{d\Delta F}{dt} = \Phi. \quad (1)$$

In this expression,  $d\Delta F/dt$  is the gain of free energy when the pore is growing (a quantity we count positively when the energy decreases, and negatively, otherwise) and  $\Phi$  is the dissipated energy (per unit time).

We give now the expression for the different terms. Let  $r$  be the radius of the dislocation loop (in practice, a pore) at time  $t$  and  $r_i$  its initial radius (at time  $t=0$ ).

The free energy gained per unit time  $d\Delta F/dt$  contains three terms.

(i) The energy of creation of the dislocation  $-2\pi E(dr/dt)$  (with  $E$  the line tension of the dislocation and the minus sign is because creating the dislocation costs energy).

(ii) The decrease of surface energy  $-\gamma(dS/dt)$  (with  $\gamma$  as the surface tension and  $S$  as the surface area of the whole system, which tends to decrease in time); this term also equals  $(\gamma/R)(dV_m/dt) = (\gamma/R)2\pi r d(dr/dt)$ , with  $V_m$  as the volume of the meniscus and  $R$  as its radius of curvature (note that  $\Delta P_m = P_{air} - P_m = \gamma/R$  with  $R > 0$  is the pressure drop inside the meniscus with respect to the atmospheric pressure, caused by its surface curvature [5]).

(iii) The decrease in surface interaction energy when the pore is created  $2\pi r(dr/dt)[f(Nd) - f((N-1)d)]$  where  $f$  is, by definition, the interaction energy per unit surface area between the free surfaces (taken equal to 0 when the number  $N$  of layers in the film, tends to infinity). Note the implicit assumption that the Burgers vector of the dislocation is equal to the layer thickness  $d$  (elementary dislocation).

The dissipation  $F$  also contains three terms.

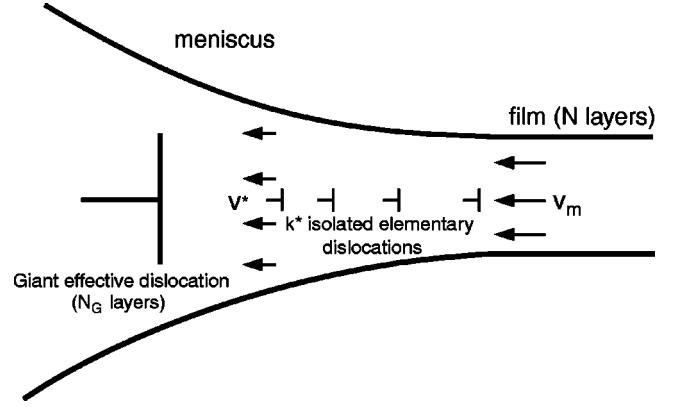


FIG. 2. Model of meniscus (schematic) used to represent the behavior of the real meniscus.

(i) The energy dissipated by the flow around the core of the dislocation in the film  $\Phi_d$ , which we usually write in the form  $2\pi r(d/\mu)(dr/dt)^2$ , with  $\mu$  as the mobility of the dislocation (note that in Ref. [11] we called  $1/\mu$  as the mobility of the dislocation). Hydrodynamic calculations show that  $m \approx (\lambda_p/\eta)^{1/2}$  [13], where  $\lambda_p$  is the permeation coefficient and  $\eta$  is the shear viscosity parallel to the layers ( $\eta_3$  in the Martin-Parodi-Pershan notation, see Ref. [12], p. 83), in good agreement with the metallurgical model [14,15]. The hydrodynamical model predicts that the mobility of a dislocation should be independent of its Burgers vector [12], a claim that has not yet been checked experimentally, but which we will use in the following. Note, in addition, that  $\mu$  is independent of  $N$  in thick films but is predicted to decrease in thin films as  $\mu(N-1)/N$  (the mobility in an infinite medium is denoted by  $\mu$ ) (for a demonstration, see Ref. [12], p. 104). Because of the dependence on  $N$ , this confinement effect becomes significant in very thin films ( $N < 10$ ). The mobility  $\mu$  has also been measured directly from creep experiments of the smectic phase compressed between to glass plates [6,12].

(ii) The energy  $\Phi_m$  dissipated by the flow in the meniscus, which can be expressed in the form  $2\pi r_m C N d v_m^2/\mu$ , where  $C$  is a function of  $N$  which has been estimated in Ref. [11], and  $v_m = (1/N)(r/r_m)(dr/dt)$  the average hydrodynamic velocity at the entrance of the meniscus (see Fig. 2).

(iii) The energy  $\Phi_f$  dissipated by the bidimensional flow inside the film. This contribution equals  $4\pi\eta dr^2(dr/dt)^2(1/r^2 - 1/r_m^2)/N$  (here  $\eta$  denotes the shear viscosity in the plane of the layers, i.e.  $\eta_2$  in the Martin-Parodi-Pershan notation, see Ref. [12] p. 83) [10]. This term is completely negligible with respect to  $\Phi_d$  (by a factor 500 at least). We shall therefore neglect it in the following.

Finally, Eq. (1) can be rewritten in the form [10]

$$\frac{1}{\mu} \frac{dr}{dt} \left( 1 + \frac{Cr}{r_m N} \right) = \frac{\gamma}{R} + \frac{f(Nd) - f((N-1)d)}{d} - \frac{E}{rd}. \quad (2)$$

This formula generalizes Eq. (5) given in Ref. [11] as it now takes into account the interactions between the free surfaces [second term in the right-hand side (rhs) of the equation]. This equation allows us to calculate the radius of nucleation of a pore:

$$r_c = \frac{E}{d\Delta P_m + f(Nd) - f((N-1)d)}. \quad (3)$$

Equation (2) can be solved analytically. By introducing the characteristic time

$$t_c = \frac{dr_c}{\mu[d\Delta P_m + f(Nd) - f((N-1)d)]}, \quad (4)$$

its solution may be expressed as

$$\frac{t}{t_c} = \left(1 + \frac{Cr_c}{r_m N}\right) \left[\frac{r-r_i}{r_c} + \ln\left(\frac{r-r_c}{r_i-r_c}\right)\right] + C \frac{r^2 - r_i^2}{2r_m r_c}, \quad (5)$$

where  $r_i$  is the pore radius at the initial time  $t_i$ .

This expression allows us to predict the growth dynamics of a pore in a smectic film. It depends on physical quantities which can be measured experimentally.

(i) The radius  $r_m$  of the meniscus and its radius of curvature  $R$ , both measurable with a reflected light microscope [5].

(ii) The number  $N$  of layers in the film, also measurable within one layer by reflectivity.

(iii) The initial radius  $r_i$  at time  $t_i$  (defined within a constant), which must be larger than  $r_c$  to avoid the loop collapse (in practice,  $r_i$  is two to many hundreds times larger than  $r_c$  and strongly depends on the film thickness and on the nucleation process [5], for details, see the following paragraph).

(iv) The constant  $C$ , which can be measured as a function of  $N$  by equilibrating two meniscus of different sizes [10,12,16]. Theoretically, it is given by the following formula [11]:

$$C(N) = \frac{k^*}{k^* + N} + N_G \frac{N}{(N + k^* - 1)^2}, \quad (6)$$

where  $N_G$  is a constant and  $k^*$  is a function of  $N$  given by

$$k^*(N + k^*)^4 = \frac{4l_p^2 R}{d^3}, \quad (7)$$

where  $l_p$  is the permeation length ( $l_p = \sqrt{\lambda_p \eta_3}$ ). From a physical point of view, we decompose the dislocations of the meniscus into two groups: a first one of  $k^*$  dislocations which can be considered as isolated from a hydrodynamical point of view, and a second one containing all the other dislocations. Because the dislocations of the second group are too close to each other to be considered as isolated, they are replaced in the model by a giant dislocation of effective Burgers vector  $N_G d$  (Fig. 2). As a consequence, the first term in the rhs of Eq. (6) represents the dissipation caused by the permeation flow around the  $k^*$  isolated dislocations, while the second term corresponds to the dissipation associated with the flow around the effective giant dislocation. In practice, the first term in the rhs of Eq. (6) always dominates the other and  $N + k^* - 1 \gg 1$ . As a consequence, Eq. (6) simplifies in the form

$$C(N) \approx N_G \frac{N}{(N + k^*)^2}, \quad (8)$$

with  $k^*$  given by Eq. (7). As we shall see later in Sec. III,  $C(N)$  has a maximum when  $k^*$  goes to zero, i.e., when it is no longer possible to consider any dislocation as isolated. This condition allows us to calculate from Eqs. (7) and (8) the values of  $N$  and  $C$  at the maximum of the curve  $C(N)$ :

$$N_{max} = \left(\frac{4l_p^2 R}{d^3}\right)^{1/4}, \quad (9)$$

$$C_{max} = \frac{N_G}{N_{max}}. \quad (10)$$

Finally, the model predicts that when  $N \gg N_{max}$ , the constant  $C$  must decrease asymptotically as

$$C(N) \approx \frac{N_G}{N}. \quad (11)$$

The function  $f$ , representing the interaction free energy, can be obtained by measuring the apparent matching angle  $\theta_m$  between the meniscus and the film [8]:

$$2\gamma(\cos \theta_m - 1) = f(H). \quad (12)$$

Previous measurements have showed that the main contribution to  $f(H)$  is due to the enhancement of the smectic order parameter at the free surfaces: this order excess exponentially decays within the film thickness over a distance that is given by the smectic correlation length  $\xi$ . The angle  $\theta_m(H)$  can be calculated from a Landau-de Gennes mean-field theory [8,10,12], which turns out to fit very well with the experimental data. As such, we use our experimental values of  $\theta_m$  to calculate the values of  $f(H)$  [Fig. 3(a)]. Note that in this figure,  $f(H) \approx 0$  for  $N \geq 10$ , because in ‘‘thick’’ films, the matching between the film and the meniscus is tangential within the experimental error ( $\theta_m \approx 0$ ). These results were recently confirmed by Jaquet and Schneider who obtained the function  $f(H)$  by directly measuring the film tension  $\tau$  at different thicknesses. We recall that the film tension reads [8]

$$\tau(H) = 2\gamma + \Delta P_m H + f(H). \quad (13)$$

Thus, the function  $f(H)$  can be obtained by subtracting from  $\tau(H)$  the linear term  $2\gamma + \Delta P_m H$  extrapolated from measurements in thick films [where  $f(H) \approx 0$ ]. Jaquet and Schneider [17] fitted all their 8CB data to the trial function (for  $T < 30^\circ\text{C}$ )

$$f(Nd) = -\frac{K}{(T_{NA} - T)^\kappa} \exp\left(-\frac{Nd}{\sqrt{2}\xi}\right), \quad (14)$$

with  $K = 2.936$  CGS,  $\kappa = 0.316$ , and  $d/\sqrt{2}\xi = 1.007$ . This function is plotted in Fig. 3(a) for  $T = 28.7^\circ\text{C}$  ( $T_{NA} - T = 4.7^\circ\text{C}$ ) and turns out to be close to our experimental values. Note that our data can as well be fitted with the same

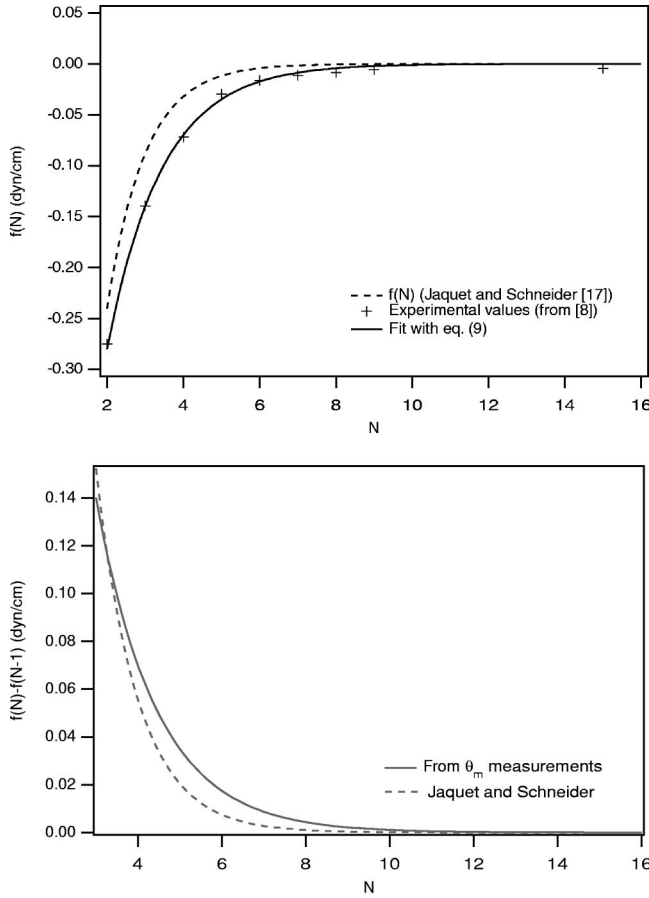


FIG. 3. (a) Interaction energy as a function of the film thickness. The dotted line corresponds to the measurements of Jaquet and Schneider [17]. The solid line is the best fit to Eq. (13) of our experimental data obtained from the measurement of the apparent contact angle [8]. (b) Force acting on the dislocation due to surface interactions.

function by taking  $K=1.873$  CGS,  $\kappa=0.330$  and  $d/\sqrt{2}\xi = 0.695$ . These are the values we have chosen in the following. Note that the force on the dislocation due to surface interactions is given by the difference  $f(N) - f(N-1)$ . The values of this force are fairly close when using our data or those of Jaquet and Schneider, as illustrated in the graph of Fig. 3(b);

Finally, we need to know the surface tension  $\gamma$  (which has been measured very precisely, see Refs. [17,18]), the pressure difference  $\Delta P_m$ , given by the usual Laplace law [5], which requires a measurement of the radius of curvature  $R$  of the meniscus), and the line tension  $E$  of the dislocation, measured previously in the gravity field of a vertical film and shown to depend on the film thickness as follows [7]:

$$E(N) = E_\infty + \frac{\delta E}{\sqrt{N+1/2}}. \quad (15)$$

Because all of these quantities are known experimentally (except for  $C$ , which has been estimated in Ref. [10]), we can, in principle, predict the time evolution of a pore for any

film thickness  $H=Nd$ , pressure difference  $\Delta P_m$ , and initial radius  $r_i$ . Before doing this, we first describe our experimental results.

### III. DISLOCATION LOOP DYNAMICS: EXPERIMENTAL

All our experiments were performed with 4-*n*-octylcyanobiphenyl (8CB) from Merck Ltd. The films are stretched over a circular frame and placed inside an oven regulated within  $\pm 0.05$  °C. The frame is simply a circular hole made in a 1-mm-thick plate and beveled on the sides. The radius of the meniscus is  $r_m=1.5$  mm. Its radius of curvature  $R$  and the film thickness  $H$  are measured by interferometry. After preparation, the film is kept at rest for 1 day, this time being necessary to eliminate all the dislocations in the film and to equilibrate the pressure inside the meniscus. After this equilibration time, a loop is nucleated in the middle of the film with the help of a very small heating wire placed  $50 \mu\text{m}$  under the film [5]. A very short current pulse in the wire allows us to locally heat the film for a few milliseconds slightly above its spontaneous thinning transition temperature  $T(N)$  [5,8,10,12]. After the end of the pulse, the temperature rapidly decreases (in less than 1 s) and restabilizes to the temperature of the oven. Note that the diffusion time of heat in the heating wire is of the order of  $\tau_H \approx l^2/D$ , where  $l$  is the size of the wire and  $D$  is the heat diffusion coefficient. In a metal  $D \approx 1 \text{ cm}^2/\text{s}$ , which gives  $\tau_H \approx 10^{-2}$  s by taking  $l=1$  mm. As a consequence, we consider that the relaxation time of the temperature inside the oven after the nucleation is less than 1 s. This estimate is confirmed by the observation of the nucleation process with a rapid camera (see Fig. 4). It may happen that the pulse is too short; in that case, the loop radius  $r_i$  after the temperature restabilization is less than the critical radius  $r_c$  calculated at the oven temperature, so that the loop collapses. By increasing the duration of the pulse (or, preferably, the power), it is possible to exceed the critical radius above which the loop grows. Its dynamics is then recorded after the temperature is stable.

In spite of its apparent simplicity, this experiment is difficult to perform. The first reason is that it is preferable to measure the curves  $r(t)$  with the same film, because, in this case, the meniscus does not change ( $\Delta P_m$  can be considered as a constant, which, of course, requires there is no leak of material on the frame). Second, it is necessary to wait at least half a day between two measurements: indeed, each loop must join the meniscus before another is nucleated and a new  $r(t)$  curve is recorded. This condition is fundamental to obtain reproducible results and was first found experimentally (it will be explained in the following section). Also complicating matters is the fact that the film can break very easily each time a loop is nucleated. As a consequence, succeeding in getting thinner the same film from  $N=300$  to  $N=3$  is not so easy to maintain, especially when the film becomes very thin as it is necessary to heat it strongly to nucleate a loop. This operation even becomes perilous when  $N < 10$  because the temperature must be increased by more than  $15$  °C above  $T_{NA}$ ; the film then locally melts into the isotropic phase, as observations with a rapid camera (1000 images per second) have shown [10] (Fig. 4). In that case, the local heating is

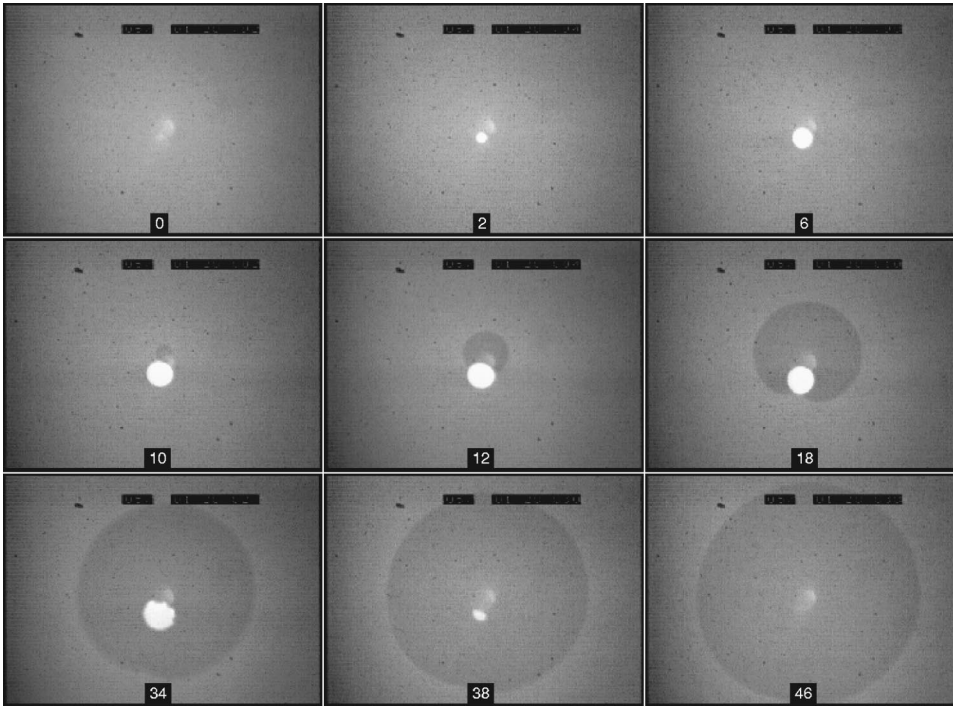


FIG. 4. Observation with a fast camera of the nucleation process in a film of eight layers. Time is given in milliseconds on each picture. At the end of the sequence the isotropic droplet which forms first (white spot) has completely disappeared, leaving a pore of large size ( $400 \mu\text{m}$  in radius). The heating wire placed under the film appears as a diffused white spot visible in all pictures.

large and the loop grows very fast during the thermal transient regime, which prevent us from recording at the set temperature (i.e., at the temperature of the oven) the beginning of the growth process (in practice below a radius of about  $400 \mu\text{m}$ ).

In Figs. 5(a) and 5(b), we have plotted the experimental curves  $r(t)$  for different values of  $N$  in two different films. The temperature of the oven was fixed to  $28.4^\circ\text{C}$  (at this temperature  $\gamma \approx 30.6 \text{ erg/cm}^2$  [17,18]). In each case, the pressure inside the meniscus was constant, with  $\Delta P_m \approx 260 \text{ dyn/cm}^2$  in Fig. 5(a) ( $R=0.117 \text{ cm}$ ) and  $\Delta P_m \approx 110 \text{ dyn/cm}^2$  in Fig. 5(b) ( $R=0.275 \text{ cm}$ ). The origin of time is arbitrary for each curve (and has been chosen in order that the curves do not intersect). Note that the time range in Fig. 5(a) corresponding to thick films ( $N > 20$ ) is much wider than in Fig. 4, corresponding to very thin films ( $N < 10$ ), although the radius variations are comparable.

These two sets of curves show three essential results.

(i) In thick films (more than 100 layers, typically),  $r(t)$  linearly increases in time (as long as  $r \gg r_c$ ), independently of the pore size. The velocity  $v = dr/dt$  is constant and will be denoted by  $v_\infty$  in the following. In addition, we have verified that, within the experimental error,  $v_\infty$  is proportional to  $\Delta P_m$ , as already shown in Refs. [5,6]. Indeed,  $v_\infty/\Delta P_m$  (which gives the mobility  $\mu$  of the dislocation in an infinite medium) equals  $4(\pm 0.5)10^{-7} \text{ cm}^2 \text{ s/g}$  in Fig. 5 (curves  $N=139$  and  $N=208$ ). This value of the mobility is in agreement with that found previously in 8CB at  $28^\circ\text{C}$  ( $\mu \approx 4.410^{-7} \text{ cm}^2 \text{ s/g}$  [6]).

(ii) In films of intermediate thicknesses (between 100 and 10 layers, typically), the growth velocity is systematically smaller than  $v_\infty$  and decreases in time when  $r$  approaches the radius of the meniscus.

(iii) For thin films (less than ten layers), the velocity is globally larger than  $v_\infty$ , an effect that becomes important in

very thin films as shown in Fig. 4. Nevertheless, the velocity still decreases in time when  $r$  approaches  $r_m$ .

#### IV. COMPARISON BETWEEN THEORY AND EXPERIMENT

In Figs. 5(a) and 5(b), we have plotted the experimental curves  $r(t)$  from Eq. (5) for the different values of  $N$ . Fit parameters are the constant  $C$  (characterizing the dissipation in the meniscus) and the initial time  $t_i$  (which, in practice, never differs by more than 1 s from the experimental value). Because our experiments were all performed at  $T = 28.5^\circ\text{C}$ , we used experimental values of the parameters at this temperature. For  $f(H)$ , they are given in Fig. 1(b); for the mobility of the dislocation we have taken the value obtained from creep experiments in compression normal to the layers  $\mu = 4.510^{-7} \text{ cm}^2 \text{ s/g}^{-1}$  [6]: for the surface tension,  $\gamma \approx 30.5 \text{ erg/cm}^2$  [17,18]; for the line tension [given in Eq. (15)],  $E_\infty = 4.510^{-7} \text{ dyn}$  and  $\delta E = 1.310^{-6} \text{ dyn}$  according to previous measurements in vertical films [7]. Finally, values of  $C$  obtained by fitting the experimental curves  $r(t)$  are given in Fig. 6 (squares and circles). To complete this set of data, we have added a few results obtained from preliminary measurements consisting of equilibrating two meniscus of different radii [16]. The values obtained in this way are close to those deduced by fitting the  $r(t)$  curves (crosses in Fig. 6). Finally, we plot the curve  $C(N)$  using Eqs. (6) and (7). The fit parameters are the permeation length  $l_p$  [fixing the function  $k^*(N)$  used in Eq. (6) where we have taken  $R = 0.117 \text{ cm}$ ] and the Burgers vector (given by  $N_G d$ ) of the giant dislocation representing the main part of the meniscus. From this fit we obtained  $l_p \approx 15 \text{ \AA}$  (two times the distance between two molecules in a layer) and  $N_G \approx 58\,000$ , which gives  $N_G b = 170 \mu\text{m}$ . This last value appears very large as it is comparable to the total height of the meniscus in contact

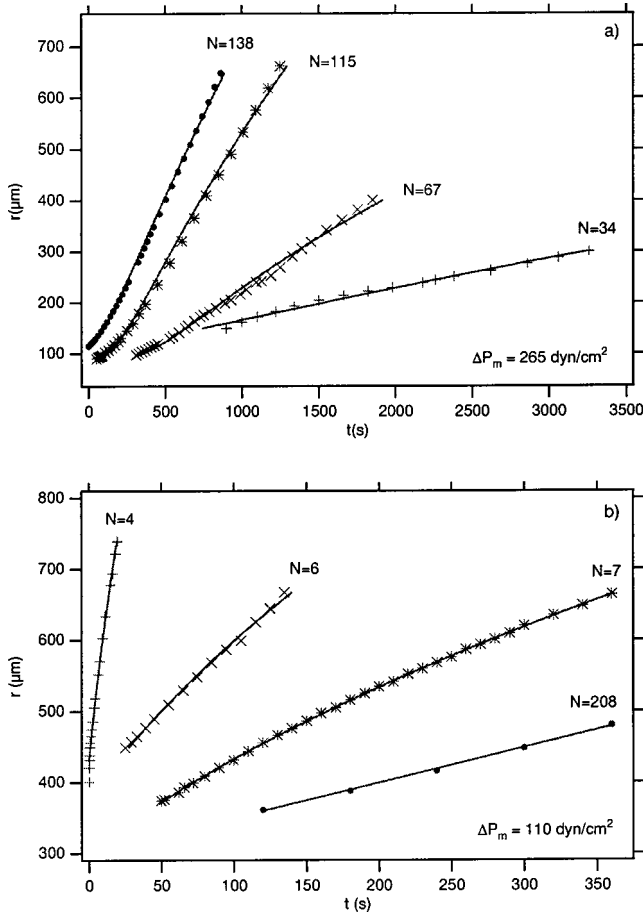


FIG. 5. Curves  $r(t)$  measured after the transient thermal regime in two different films. In (a) we show curves obtained for large and intermediate values of  $N$  ( $\Delta P_m \approx 260$  dyn/cm<sup>2</sup>,  $N > 20$ ); in (b) values of  $N$  are much smaller ( $\Delta P_m \approx 110$  dyn/cm<sup>2</sup>,  $N < 10$ ). Only a part of the curve measured at  $N=208$  is shown for comparison. In both graphs the curves have been shifted in time in order that they do not cross. The solid lines are the best fits obtained from Eq. (5) by taking the values of  $C$  given in Fig. 6.

with the frame. This means that the meniscus is a very poor reservoir of material when it changes size. This result explains our observation that equilibrating a film after stretching usually takes a very long time (1 day and sometimes more, depending on the film size, thickness and temperature).

Note that, in principle, the constant  $C$  must depend on the size of the meniscus, in particular, on its height (which, possibly, determines the value of  $N_G$ ) and, to a lesser extent, on its radius of curvature  $R$  [ $k^*(N, R)$  depending on  $R$  like  $R^{1/5}$  at small  $R$ , while  $k^* = 0$  at large  $N$ , see Eq. (6)]. These effects could explain in part the dispersion in our experimental results.

## V. COMPARISON WITH SOAP FILMS OBTAINED FROM CONCENTRATED MICELLAR SOLUTIONS

It has been known for a very long time that the drainage of thin soap films made from concentrated surfactant solutions occurs in steps [19,20]. “Thin” means that the film

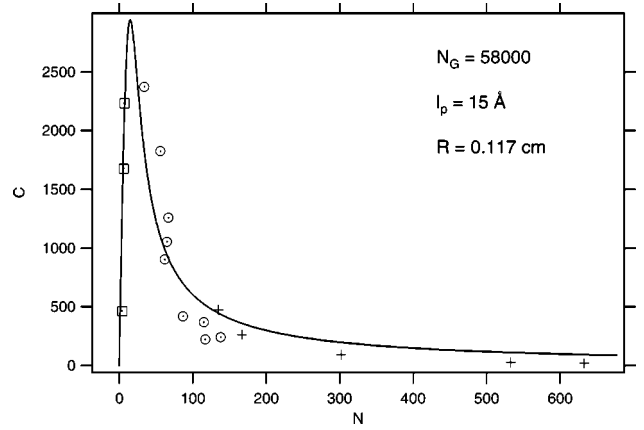


FIG. 6. Values of  $C$  obtained as a function of  $N$  by fitting the experimental curves  $r(t)$  with Eq. (5) (squares and dots). Points which are given for large values of  $N$  (crosses) have been recently obtained by another method consisting of equilibrating two menisci of different radii. The solid line is the best fit obtained from Eqs. (6) and (7).

thickness is typically less than 100 nm. In this case, surfactant molecules form charged micelles which arrange into layers as in the smectic phase (because charged micelles repel each other) [21–23]. It was shown that, when the film contains more than two or three layers of micelles, pores spontaneously nucleate inside and grow according to a diffusive law  $r \approx \sqrt{D_{eff}t}$  with  $D_{eff} \approx 10^{-8}$  cm<sup>2</sup>/s [24]. This law comes from a balance between the disjoining pressure force due to van der Waals interactions between the free surfaces (the driving force, as in very thin smectic films, with the difference that in smectics, the force is mainly due to the enhancement of the smectic order at the air interface) and the viscous force, associated to the “Poiseuille” flow of matter within the film thickness. This interpretation leads to the following formula:

$$D_{eff} = -\frac{H^3}{3\mu} \frac{\partial \Pi_d}{\partial H}, \quad (16)$$

where  $\Pi_d$  is the disjoining pressure,  $\mu$  is the viscosity of the liquid, and  $H$  is the film thickness. This formula (also used in the context of the dewetting of a liquid on a solid substrate [25]) gives values of  $D_{eff}$  in good agreement with the experiments [24]. It must be emphasized that this dissipation mechanism is different from the one that is relevant to our experiments with smectics, where permeation plays a dominant role, both locally around the core of the looped dislocation and in the bulk of the meniscus. (The meniscus can be considered to be a “perfect” reservoir in surfactant solutions, in contrast to the smectic case.)

## VI. CONCLUSION

We have shown that loop dynamics in freestanding films of smectic-A phase strongly depends on the film thickness. If the film is thick ( $N > 100$ ), the growth velocity of the loop is given by its local mobility and by the pressure difference imposed by the meniscus. In this case, the meniscus acts as a

perfect reservoir. In films of intermediate thicknesses ( $10 < N < 100$ ), a new phenomenon occurs: the growth velocity decreases when the radius of the loop approaches that of the meniscus. This effect is due to the finite permeability of the meniscus, which acts as a dissipative reservoir. This can considerably disturb the loop dynamics, especially when the film thickness is close to 30 layers. In very thin films ( $N < 10$ ), another new effect adds to the previous ones: the free surfaces attract each other, which exerts an additional driving force on the dislocation. As a result, its growth velocity strongly increases and is only fixed by the force due to the strong interaction between the surfaces ( $\Delta f \gg d\Delta P_m$ ). Because this interaction is caused by the enhancement of the smectic order parameter at the free surfaces, it exponentially decreases with film thickness, and as such plays a significant role only when  $N < 10$ . In this range of thicknesses, the slowing down of the loop is still visible when its radius becomes comparable to that of the meniscus.

In the future, we plan to measure more accurately the constant  $C$ . One experiment currently in progress consists of measuring the equilibration time of two meniscus of different

sizes connected by a film of a given thickness. This method is reliable for very thick films (more than 100 layers) but is difficult to use with thin films, because it takes too much time. For this reason, two other experiments are envisaged, consisting of measuring, either the pressure inside a bubble when it is blown up from a plane film [26], or the quality factor of the resonance peak of a vibrating film [3,27]. In these two experiments, the finite permeability of the meniscus should play a major role which has not yet been investigated experimentally. Finally, it would be interesting to look at the dynamics of dislocation loops in films where the surface layers have crystallized. In this case, we expect a strong slowing down due to the flow of matter inside the film thickness and a  $\sqrt{t}$  growth law, such as that observed in soap films (provided this dissipation mechanism dominates the others, which is possible in thin films).

#### ACKNOWLEDGMENT

The authors would like to thank Dr. Vance Bergeron for a very fruitful discussion about soap films.

- 
- [1] P.S. Pershan, *Structure of Liquid Crystal Phases* (World Scientific, Singapore, 1988).
- [2] G. Friedel, *Ann. Phys. (Paris)* **18**, 273 (1922).
- [3] P. Pieranski, L. Beliard, J.Ph. Tournellec, X. Leoncini, C. Furtlehner, H. Dumoulin, E. Riou, B. Jouvin, F.P. Fénerol, Ph. Palaric, J. Heuving, B. Cartier, and I. Kraus, *Physica A* **194**, 364 (1993).
- [4] L. Lejcek and P. Oswald, *J. Phys. II* **1**, 931 (1991).
- [5] J.C. Géminard, R. Holyst, and P. Oswald, *Phys. Rev. Lett.* **78**, 1924 (1997).
- [6] F. Picano, R. Holyst, and P. Oswald, *Phys. Rev. E* **62**, 3747 (2000).
- [7] For measurements of the line tension see J.C. Géminard, C. Laroche, and P. Oswald, *Phys. Rev. E* **58**, 5923 (1998); A. Zywockinski, F. Picano, P. Oswald, and J.C. Géminard, *ibid.* **8133**, 8133 (2000).
- [8] F. Picano, P. Oswald, and E. Kats, *Phys. Rev. E* **63**, 021705 (2001).
- [9] A. Poniewierski, P. Oswald, and R. Holyst, *Langmuir* **18**, 1511 (2002).
- [10] F. Picano, Ph.D. thesis, Ecole Normale Supérieure de Lyon, 2001 (unpublished), order no. 198.
- [11] P. Oswald, P. Pieranski, F. Picano, and R. Holyst, *Phys. Rev. Lett.* **88**, 015503 (2002).
- [12] P. Oswald and P. Pieranski, *Les Cristaux Liquides: Concepts et Propriétés Physiques Illustrés par des Expériences* (Gordon & Breach Science, New York, 2002), Vol. 2.
- [13] Orsay Group, *J. Phys. (France)* **36**, C1-305 (1975).
- [14] C.E. Williams and M. Kléman, *J. Phys. (France) Lett.* **35**, L33 (1974).
- [15] R. Holyst and P. Oswald, *Int. J. Mod. Phys. B* **9**, 1515 (1995).
- [16] F. Caillier and P. Oswald (unpublished).
- [17] R. Jaquet and F. Schneider, *Phys. Rev. E* **67**, 021707 (2003).
- [18] F. Schneider, *Rev. Sci. Instrum.* **73**, 114 (2002).
- [19] E.S. Johnnot, *Philos. Mag.* **11**, 746 (1906).
- [20] J. Perrin, *Ann. Phys. (Paris)* **10**, 160 (1918).
- [21] P.A. Kralchevsky, A.D. Nikolov, D.T. Wasan, and I.B. Ivanov, *Langmuir* **6**, 1180 (1990).
- [22] V. Bergeron and C.J. Radke, *Langmuir* **8**, 3020 (1992).
- [23] V. Bergeron, A.I. Jiménez-Laguna, and C.J. Radke, *Langmuir* **8**, 3027 (1992).
- [24] A.A. Sonin and D. Langevin, *Europhys. Lett.* **22**, 271 (1993).
- [25] J.F. Joanny and P.G. de Gennes, *J. Phys. (Paris)* **47**, 121 (1986).
- [26] P. Oswald, *J. Phys. (Paris)* **48**, 897 (1987); R. Stannarius and C. Cramer, *Liq. Cryst.* **23**, 371 (1997); *Europhys. Lett.* **42**, 43 (1998); R. Stannarius, C. Cramer, and H. Schring, *Mol. Cryst. Liq. Cryst. Sci. Technol., Sect. A* **329**, 1035 (1999); *Mol. Cryst. Liq. Cryst. Sci. Technol., Sect. A* **350**, 297 (2000).
- [27] K. Miyano, *Phys. Rev. A* **26**, 1820 (1982); C. Even, Thèse de doctorat, Université de Paris-Sud, 1999.